Performance improvement in pentacene organic thin film transistors by inserting a C_{60} ultrathin layer*

Sun Qin-Jun(孙钦军)†, Xu Zheng(徐 征)‡, Zhao Su-Ling(赵谡玲), Zhang Fu-Jun(张福俊), and Gao Li-Yan(高利岩)

Institute of Optoelectronics Technology, Beijing Jiaotong University, Beijing 100044, *China*
Key Laboratory of Luminescence and Optical Information (Beijing Jiaotong University), Ministry of Education, Beijing 100044, China

(Received 26 April 2010; revised manuscript received 11 June 2010)

The contact effect on the performances of organic thin film transistors is studied here. A C_{60} ultrathin layer is inserted between Al source–drain electrode and pentacene to reduce the contact resistance. By a 3 nm C_{60} modification, the injection barrier is lowered and the contact resistance is reduced. Thus, the field-effect mobility increases from 0.12 to 0.52 $cm^2/(V{\cdot}s)$. It means that inserting a C_{60} ultra thin layer is a good method to improve the organic thin film transistor (OTFT) performance. The output curve is simulated by using a charge drift model. Considering the contact effect, the field effect mobility is improved to 1.15 $cm^2/(V{\cdot}s)$. It indicates that further reducing the contact resistance of OTFTs should be carried out.

Keywords: organic thin film transistors, field effect mobility, contact effect, charge drift
PACS: 73.61.Ph **DOI:** 10.1088/1674-1056/20/1/017306

1. Introduction

Organic thin film transistors (OTFTs) have experienced unprecedented progress in recent years due to their potential applications in low-cost, large-area flexible displays and low-end electronics.[1−8] However, the currently developed OTFTs still have some disadvantages, such as large contact resistance, low carrier mobility and high operating voltage.[9−13] The fundamental origin of the contact resistance is still unclear, which could be minimized by using long-channel devices and/or highly doped contacts as inorganic field effect transistors. Generally speaking, the contact resistance of P-type OTFTs arises from the mismatch of energy level and the interface interaction between source–drain (S–D) electrodes and the organic semiconductor.[14−16]

The switching speed (cut-off frequency) of OTFTs is only 0.1–1 MHz, which comes to be the bottleneck for the applications of OTFTs. For example, radio frequency identification tags require the switching speed of OTFTs at 13 MHz. As we know, the switching speed of OTFTs is inversely proportional to the channel length (L) square. However it must be careful to avoid the resistance-limited contact in OTFTs when L is shrunk. Thus, ongoing contact engineering efforts to make lower resistance contacts to organic semiconductor will become more and more important for OTFTs development and the advancement of organic electronics.[17−21]

In the present paper, a series of bottom-gated top-contact pentacene devices with Al as source and drain electrode modified by a C_{60} ultrathin layer is fabricated. By modification, the field effect mobility of the OTFT is greatly improved. Then, a compact model—charge drift model is used to simulate the output characteristics and a correct extraction of the maximum of the field-effect mobility is found. Finally, the contact resistances of the OTFTs are measured and the model is proved to well simulate devices with low injection barrier.

2. Experiment

The schematic diagram of pentacene OTFTs is shown in Fig. 1. The devices were fabricated on highly doped n^+-Si wafer substrates with a 300 nm

*Project supported by the National Natural Science Foundation of China (Grant Nos. 10774013, 10974013, 60978060 and 10804006), the Research Fund for the Doctoral Program of Higher Education, China (Grant Nos. 20090009110027, 20070004024 and 20070004031), the Beijing Municipal Science and Technology Commission (Grant No. 1102028), and the National Basic Research Program of China (Grant No. 2010CB327704).
†E-mail: sunqinjun8888@163.com
†Corresponding author. E-mail: zhengxu@bjtu.edu.cn
© 2011 Chinese Physical Society and IOP Publishing Ltd

thermally grown oxide layer. The substrates ware ultrasonically cleaned sequentially in acetone, alcohol and deionized water (18 MΩ). Then a 40 nm pentacene layer was thermally evaporated in a high vacuum of 1×10^{-4} Pa through self-organizing process in the evaporation chamber for organic materials. The samples were next transported into the evaporation chamber for inorganic materials through the transport chamber by manipulator hands. The transport process was in a vacuum of 2×10^{-1} Pa. Finally, C_{60} and Al were evaporated through a metal shadow mask that had been manipulated before transportation. To improve the crystallization, the devices were annealed in a N_2-filled glovebox (O_2, H_2O< 0.1 ppm) at normal pressure (1 atm) and 100 ° for half an hour.[22−24] The parameters of our fabrications are shown in Table 1.

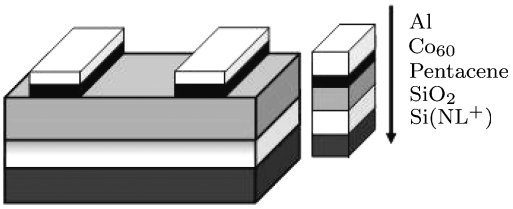


Fig. 1. Schematic diagrams of OTFTs.

The electrical characteristics of the OTFTs were then measured in air and at room temperature by using the KEITHLEY *I*–*V* System. This system consists mainly of KEITHLEY2612, K EITHLEY2410 and LPT probe station.

Table 1. Fabrication parameters of OTFTs.

	evaporating vacuum/ Pa	rotating speed of substrate/rpm	rate of deposition /nm·s^{-1}	thickness of film/nm	material purity
SiO_2	—	—	0.1	170	99.99%
Pentacene	1×10^{-4}	12	0.01–0.03	40	98%
C_{60}	2×10^{-3}	20	0.003–0.01	0, 1, 3, 5	99%
Al	2×10^{-3}	20	0.5–1	120	99%

3. Results and Discussion

Figure 2(a) shows the curves for source–drain current (I_{DS}) at different values of gate voltage (V_{GS}) versus source–drain voltage (V_{DS}) of the OTFTs whose S–D electrodes are modified by 3 nm C_{60}. The device shows typical p-channel characteristics. Due to the big contact resistance, I_{DS} is very small at low voltages. The electrical transfer characteristics are shown in Fig. 2(b), from which we can obtain the V_T value to be −7.6 V.

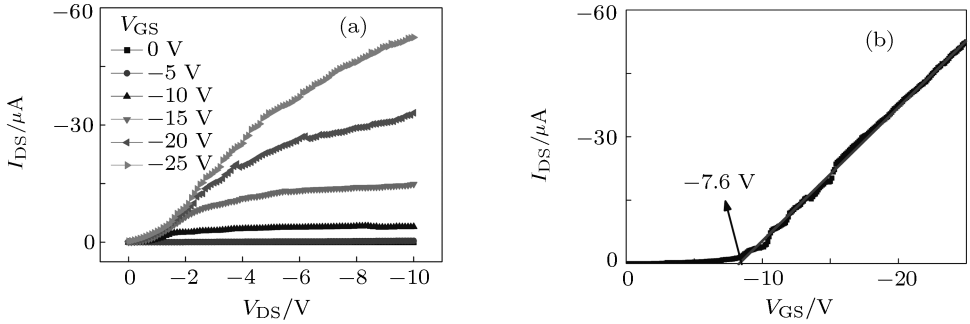


Fig. 2. (a) Output characteristics and (b) transfer characteristics of OTFT device with a 3 nm C_{60} modifying Al as source and drain electrode.

At present, the metal–oxide–semiconductor field-effect transistor (MOSFET) model is used to describe OTFTs.[25−28] In the gradual channel approximation, the expression of I_{DS} is

$$I_{DS} = \frac{WC_i\mu_{ef}}{L}\left[(V_{GS} - V_T)V_{DS} - \frac{V_{DS}^2}{2}\right], \tag{1}$$

in which W is the width of transistor channel, L is the length of transistor channel, μ_{ef} is the field-effect mobility, V_T is the threshold voltage, and C_i is the capacitance per unit area of the insulator.

As we have known, a thin film transistor (TFT) always works in the linear regime when the pixel charges up in active-matrix liquid crystal display (AMLCD). Thus, here we investigate mainly the performance of OTFTs in the linear regime.

The following expression is used to describe $I_{\rm DS}$ in the linear regime:

$$I_{\rm DS} = \frac{WC_{\rm i}\mu_{\rm ef}}{L}(V_{\rm GS} - V_{\rm T})V_{\rm DS}. \quad (2)$$

The $\mu_{\rm ef}$ is extracted from the transconductance of the device, and it is defined as

$$g_{\rm m} = \frac{{\rm d}I_{\rm DS}}{{\rm d}V_{\rm GS}} = \frac{WC_{\rm i}\mu_{\rm ef}}{2L} \bullet V_{\rm DS}, \quad (3)$$

$$\mu_{\rm ef} = \frac{2L}{WC_{\rm i}V_{\rm DS}} \bullet \frac{{\rm d}I_{\rm DS}}{{\rm d}V_{\rm GS}}. \quad (4)$$

Then, we can obtain the performance of the OTFTs as listed in Table 2. The performance of devices has been improved by an ultrathin C_{60} layer modifying the S–D electrodes. The $\mu_{\rm ef}$ increases with the thickness of C_{60} increasing from 0 to 3 nm. It is in accordance with the result reported by Li *et al.*[20] They used a C_{60} ultrathin buffer layer between indium tin oxide (ITO) and pentacene and found that the work function of ITO/C_{60} increased with the C_{60} thickness increasing from 0 to 5 nm. In our experiments, the work function of bare Al is 4.2 eV and the highest occupied molecular orbital (HOMO) of pentacene is 5.0 eV. The injection barrier between Al and pentacene is 0.8 eV, which is responsible for the low $\mu_{\rm ef}$ (0.12 cm^2/(V·s)) of the OTFT devices. With the increase of C_{60} thickness, the work function of Al/C_{60} is closer to the pentacene HOMO and facilitates hole injection. The $\mu_{\rm ef}$ of the OTFT device increases to 0.52 cm^2/(V·s) at 3 nm C_{60} layer, which is nearly four times higher than that of no modifying layer. Another probable reason may be that an ultrathin C_{60} layer prevents the metal atom from diffusing into the organic layer and other chemical reactions from taking place between the organic layer and the metal.[29] However, when the C_{60} layer is thicker, it can block the carrier transport, resulting in the decrease of $\mu_{\rm ef}$.

Table 2. Performances of the OTFTs with different thicknesses of C_{60} buffer layer.

C_{60} thickness/nm	$\mu_{\rm ef}$ /(cm^2/(V·s))	$V_{\rm T}$/ V	(on/off)/10^3
0	0.12	–11.6	0.95
1	0.25	–8.2	1.0
3	0.52	–7.6	1.1
5	0.42	–9.4	1.4

Note: $W = 2.5$ mm, $L = 50$ μm, and $C_{\rm i} = 10$ nF.

We can observe from Fig. 2(a) that by a 3 nm C_{60} ultrathin layer modification, the performances of OTFTs are still affected by the contact resistance, especially at the onset voltage. Next, we use a compact model—charge drift model developed by Lara Bullejos *et al.*[30] to investigate the contact effects on OTFTs. We define a parameter $b \equiv V_{\rm C}/V_{\rm DS} = R_{\rm C}/R_{\rm T}$, which, in fact, is the ratio between contact resistance and channel resistance. Here, $V_{\rm C}$ is the contact voltage. Then the $I_{\rm DS}$ can be obtained from Eq. (1) as

$$I_{\rm DS} = \frac{WC_{\rm i}\mu_{\rm ef}}{L}\left[V_{\rm GS} - V_{\rm T} - \frac{(1+b)V_{\rm DS}}{2}\right] \times (1-b)V_{\rm DS}. \quad (5)$$

The model assumes that three phenomena occur during the charge transport through the depleted region of the OTFTs. (a) Charge carriers pass through a potential barrier at the contact, which causes the voltage for carrier injection through the barrier $V_{\rm injection}$. (b) The charged dipoles formed by the ions modulate the injection barrier and are capable of accepting other hopping electrons. These ions are created at the electrodes by a redox reaction in the organic material, thereby causing a voltage for redox process, $V_{\rm redox}$. (c) Drift of charge carriers in the bulk of the contact region causes the voltage required for charge drift $V_{\rm drift}$. Thus, the $V_{\rm C}$ can be written as

$$V_{\rm C} = V_{\rm injection} + V_{\rm redox} + V_{\rm drift}. \quad (6)$$

From Ref. [20] and the performance of the OTFTs modified by 3 nm C_{60}, it follows that the barrier height between Al and pentacene is very low, making $V_{\rm injection} \approx 0$ and $V_{\rm redox} \approx 0$.

The iterative procedure is summarized as follows. First, initial estimates of the threshold voltage and

the mobility are made by the MOSFET model. Second, as the contact effects only slightly increase the threshold voltage of the OTFTs,[31] we set the V_T to be a constant in the procedure. Third, the mobility and the voltage drop at the contact are extracted from the output characteristics by iterative procedure through using Eq. (5). The procedure is illustrated in Fig. 3 and begins with the initial values mentioned above: $\mu_0 = \mu_{ef} = 0.52$ cm^2/(V·s), and $b_0 = 0$. After four loops, a good agreement with experimental data can be obtained, where $\mu_4 = 1.15$ cm^2/(V·s), and $b_0 = 0.32$. It means that V_C is nearly one-third of V_{DS}; the correct field effect mobility of the OTFT is nearly twice the apparent value.

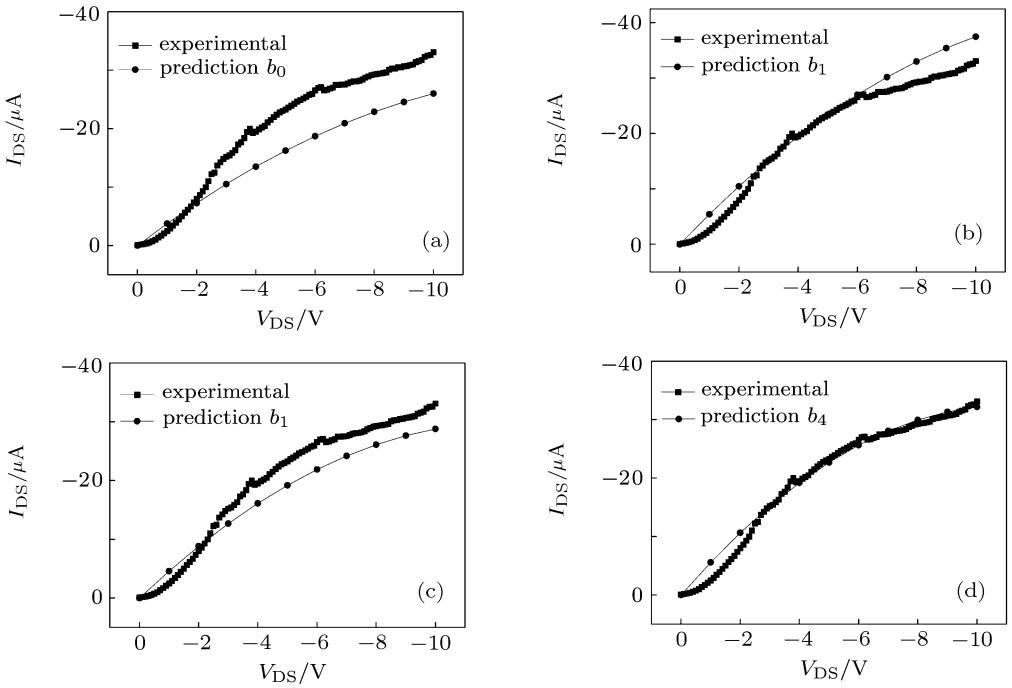


Fig. 3. Iterative procedures to fit output characteristics in the OTFTs ($V_{GS} = -20$ V), where panel (a) is for the initial values, $b = 0$, $\mu_0 = \mu_{ef}$; panel (b) for a new value b_1 obtained by fitting Eq. (5) to the experimental output characteristics in the left region (with using $\mu = \mu_0$ and varying the value of b to fit the experimental data), panel (c) for a new value μ_1 obtained by fitting Eq. (5) to the experimental output characteristics in the right region (with using $b = b_1$ and varying the value of μ to fit the experimental data) and panel (d) shows that good agreement with experimental data can be obtained after 4 loops.

Next, the contact resistance (R_c) of the OTFT devices is calculated in the linear regime. The transistor total resistance (R_{tot}) can be expressed as

$$R_{tot} = R_{ch} + R_c = \frac{L}{WC_i(V_{GS} - V_t)\mu_{ef}} + R_c, \quad (7)$$

in which R_{ch} is the channel resistance. Using the transmission line method (TLM) that is a direct application of Eq. (7), we can extract R_c values for different V_{GS} values. From Fig. 4, we can see that the R_c gate-voltage dependency is generally correlated with the increase of charge carrier concentration which introduces the current in the channel at higher V_{GS} values. The intersection with Y axis ($L \to 0$) gives the R_c value (as seen in Table 3). R_c decreases with V_{GS} increasing from -10 V to -20 V, while the value of b increases from 0.31 to 0.36.

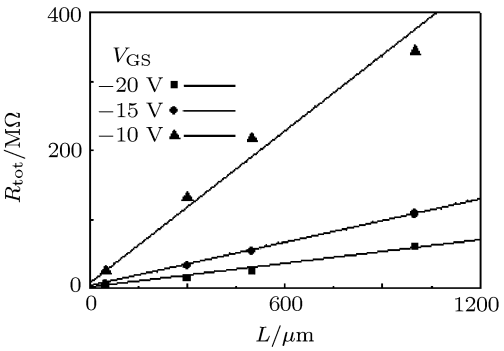


Fig. 4. Plots for total resistance R_{tot} versus channel length L of the OTFTs.

It can be seen that when V_{GS} increases, both R_c and R_L decrease with the increase of charge carrier

concentration, and R_{ch} decreases faster. This may be attributed to the non-ohmic part of R_c.[32] The value of b is 0.36 at -20 V, which is close to the model value 0.32. Thus, the charge drift model can be used in OTFTs with low injection barrier such as the device by 3 nm C_{60} modifying Al as the source and drain electrode.

Table 3. Contact resistances of the OTFTs at different values of V_{GS}.

V_{GS}/ V	R_c/MΩ	R_T/MΩ	b
–10	8.5	27.3	0.31
–15	3.6	10.8	0.33
–20	2.2	6.1	0.36

4. Conclusions

The OTFTs with bottom-gated top-contact structure are fabricated, in which a C_{60} ultrathin buffer layer is inserted between pentacene and Al electrode. After modification, the mobility of the OTFT device is improved from 0.12 to 0.52 $cm^2/(V{\cdot}s)$. Then, we use a charge drift model to simulate the $I_{DS} - V_{DS}$ curve and find that the contact effect is still a big problem that cannot be neglected. Considering the contact resistance effects could result in an correct extraction of the maximum field-effect mobility reaching 2 to 1.15 $cm^2/(V{\cdot}s)$. By the TLM, we find that the results from the charge drift model are almost in agreement with the experimental data. It indicates that the model is applicable for OTFTs with low injection barrier. Finally, the performances of OTFTs are improved by inserting an appropriate C_{60} ultrathin layer. However, the contact effect is still too big to be neglected. Further efforts to make lower resistance contacts to organic semiconductor are still important for developing OTFTs and advancing organic electronics.

References

[1] Drury C J, C. Mutsaers M J, Hart C M, Matters M and Leeuw D M 1998 *Appl. Phys. Lett.* **73** 108

[2] Gerwin G 2007 *Nature* **445** 18

[3] Crone B, Dodabalapur A, Lin Y Y, Filas R W, Bao Z, Sarpeshkar R, Katz H E and Li W 2000 *Nature* **403** 521

[4] Cao Q J, Zhang Y M, Zhang Y M, Lu H L, Wang Y H, Chang Y C and Tang X Y 2007 *Chin. Phys.* **16** 1097

[5] Tao C L, Zhang X H, Dong M J, Liu Y Y, Sun S, Ou G P, Zhang F J and Zhang H L 2008 *Chin. Phys.* B **17** 281

[6] Liu Y R, Wang Z X, Yu J L and Xu H H 2009 *Acta Phys. Sin.* **58** 8566 (in Chinese)

[7] Yuan G C, Xu Z, Zhao S L, Zhang F J, Xu N, Tian X Y and Xu X R 2009 *Chin. Phys.* B **18** 3990

[8] Boudinet D, Benwadih M, Altazin S, Gwoziecki R, Verilhac J M, Coppard R, Blevennec G L, Chartier I and Horowitz G 2010 *Org. Electron.* **11** 291

[9] Pesavento P V, Puntambekar K P, Frisbie C D, McKeen J C and Ruden P P 2006 *J. Appl. Phys.* **99** 094504

[10] Yagi I, Tsukagoshi K and Aoyagi Y 2004 *Appl. Phys. Lett.* **84** 813

[11] Minari T, Miyata Y, Terayama M, Nemoto T, Nishinaga T, Komatsu K and Isoda S 2006 *Appl. Phys. Lett.* **88** 083514

[12] Liu G, Liu M, Wang H, Shang L W, Ji Z Y, Liu X H and Liu J 2009 *Chin. Phys.* B **18** 3530

[13] Petrovic A, Pavllica E, Bratina G, Carpentiero A and Tormen M W 2009 *Synth. Met.* **159** 1210

[14] Luisier M, Schenk A and Fichtner W 2007 *Appl. Phys. Lett.* **90** 102103

[15] Halik M, Klauk H, Zschieschang U, Schmid G, Dehm C, Schütz M, Maisch S, Effenberger F, Brunnbauer M and Stellacci F 2004 *Nature* **431** 963

[16] Wang Y, Jia S, Chen Z J and Ji L J 2006 *Chin. Phys.* **15** 2297

[17] Hong I H, Lee M W, Koo Y M, Jeong H, Kim T S and Song O K 2005 *Appl. Phys. Lett.* **87** 063502

[18] Bai Y, Liu X, Chen L, Khizar-ul-Haq, Khan M A, Zhu W Q, Jiang X Y and Zhang Z L 2007 *Microelectr. J.* **38** 1185

[19] Lin Y J, Li Y C, Wen T C, Huang L M, Chen Y K, Yeh H J and Wang Y H 2008 *Appl. Phys. Lett.* **93** 043305

[20] Li Y C, Lin Y J, Wei C Y, Lin Z X, Wen T C, Chang M Y, Tsai C L and Wang T C 2009 *Appl. Phys. Lett.* **95** 163303

[21] Bao Z N and Locklin J 2007 *Organic Field-Effect Transistors* (Ohio: Chemistry Rubber Company) p155

[22] Guo D, Ikeda S, Saiki K, Miyazoe H and Terashima K 2006 *J. Appl. Phys.* **99** 094502

[23] Sekitani T, Someya T and Sakurai T 2006 *J. Appl. Phys.* **100** 024513

[24] Takenobu T, Watanabe K, Yomogida Y, Shimotani H and Iwasa Y 2008 *Appl. Phys. Lett.* **93** 073301

[25] Celle C, Suspene C, Simonato J, Lenfant S, Ternisien M and Vuillaume D 2009 *Org. Electron.* **10** 119

[26] Lee W H, Wang C C and Ho J C 2009 *Thin Solid Film* **517** 5305

[27] Kwon J H, Shin S, Kim K H, Cho M J, Kim K N, Choi D H and Ju B K 2009 *Appl. Phys. Lett.* **94** 013506

[28] Yun Y, Pearson C and Petty M C 2009 *J. Appl. Phys.* **105** 034508

[29] Chu C W, Li S H, Chen C W, Shrotriya V and Yang Y 2005 *Appl. Phys. Lett.* **87** 193508

[30] Lara Bullejos P L, Jimenez Tejada J A, Rodriguez-Bolivar S, Deen M J and Marinov O 2009 *J. Appl. Phys.* **105** 084516

[31] Street R A and Salleo A 2002 *Appl. Phys. Lett.* **81** 2887

[32] Ahnood A, Ghaffarzadeh K, Nathan A, Servati P, Li F, Esmaeili-Rad M R and Sazonov A 2008 *Appl. Phys. Lett.* **93** 163503